Research Article

Xiaohui Zhang, Yi Zhang*, Baohong Tian*, Yanlin Jia*, Yong Liu, Kexing Song, Alex. A. Volinsky, and Huihui Xue

Cr effects on the electrical contact properties of the Al_2O_3-Cu/15W composites

https://doi.org/10.1515/ntrev-2019-0012
Received Apr 24, 2019; accepted May 13, 2019

Abstract: In order to investigate the effects of chromium on the electrical contact properties of the Al_2O_3-Cu/15W composites, vacuum hot-pressing sintering and internal oxidation methods were employed to fabricate the Al_2O_3-Cu/15W and Al_2O_3-Cu/15W5Cr composites. The microstructure was analyzed by scanning and transmission electron microscopy. The electrical contacts testing was performed using the JF04C testing machine at 30 V DC with 10-30 A current. The effects of Cr on the comprehensive properties, arc erosion morphology and welding force of the electrical contacts were investigated. The mass transfer mechanism was discussed. It was demonstrated that the Al_2O_3 nanoparticles pinned dislocations. The diffraction spots of the Cu matrix and the γ-Al_2O_3 disclose an orientation relationship of $<103>_{Cu}//<103>_{\gamma-Al2O3}$,$\{020\}_{Cu}//\{040\}_{\gamma-Al2O3}$. A typical arc erosion morphology, such as needle-like and coral structures was formed, which provides significantly enhanced arc erosion resistance of the contact material. Compared with the Al_2O_3-Cu/15W composite, the Al_2O_3-Cu/15W5Cr composite has a lower welding force. The two composites present two distinct mass transfer trends before and after 25 A. The final mass transfer direction of the composites is from the cathode to the anode. The Al_2O_3-Cu/15W5Cr contacts have less mass change under all testing conditions.

Keywords: Electrical contact; Al_2O_3 nanoparticles; orientation relationship; mass transfer mechanism.

1 Introduction

Due to the manufacturing equipment upgrades and rapid development of electronics industry, vacuum switches have been playing a significant role for nearly two decades [1–3]. Currently, as the core components of vacuum switches, high-performance electrical contacts have drawn considerable attention due to their ability to reliably make and break the circuits [4–7].

Chromium, a semi-refractory metal, has a high melting point and hardness, along with a strong affinity to oxygen. Consequently, Cu-Cr electrical contacts have been used in vacuum circuit breakers, attributed to their good breaking ability and resistance to arc erosion [8–11]. Schulman *et al.* [12] reported that droplets and particles formed from the Cu-25Cr contacts during the arc erosion process. Mahir *et al.* [13] studied the effects of Cr particles with different weight ratios ranging from 5% to 15% on the properties of Cu-Cr composites, and found that the hardness and wear resistance of the composites increased significantly with chromium addition. Taylor's research [14] indicated that the cathode spot moves faster on the Cu-Cr contact when the arc changes from an initial arc column to a diffusion arc, resulting in avoiding the large-scale erosion of the contact. Considering the recent developments in large capacity vacuum switching equipment, which lead to miniaturization and high performance, a single com-

***Corresponding Author: Yi Zhang:** School of Materials Science and Engineering, Henan University of Science and Technology, Luoyang 471023, P.R. China; Collaborative Innovation Center of Nonferrous Metals, Henan Province, Luoyang 471023, P.R. China; Henan Key Laboratory of Nonferrous Materials Science and Processing Technology, Luoyang 471023, P.R. China; Email: zhshgu436@163.com

***Corresponding Author: Baohong Tian:** School of Materials Science and Engineering, Henan University of Science and Technology, Luoyang 471023, P.R. China; Collaborative Innovation Center of Nonferrous Metals, Henan Province, Luoyang 471023, P.R. China; Henan Key Laboratory of Nonferrous Materials Science and Processing Technology, Luoyang 471023, P.R. China; Email: bhtian007@163.com

***Corresponding Author: Yanlin Jia:** College of Materials Science and Engineering, Beijing University of Technology, Beijing 100124, P.R. China; Email: jiayanlin@126.com

Xiaohui Zhang, Yong Liu, Kexing Song, Huihui Xue: School of Materials Science and Engineering, Henan University of Science and Technology, Luoyang 471023, P.R. China; Collaborative Innovation Center of Nonferrous Metals, Henan Province, Luoyang 471023, P.R. China; Henan Key Laboratory of Nonferrous Materials Science and Processing Technology, Luoyang 471023, P.R. China

Alex. A. Volinsky: Department of Mechanical Engineering, University of South Florida, Tampa 33620, United States of America

ponent can no longer satisfy the increased requirements. Hence, there is a tendency to take advantage of multiple components. The research of Miao *et al.* [15] showed that adding a third component into the Cu-Cr system to form Cu-Cr-X contacts can significantly improve the resistance to arc erosion of the contacts. For example, a refractory metal, such as tungsten and molybdenum, can be added to enhance the contact's dielectric strength and arc erosion resistance. Chang *et al.* [16] studied the welding force of the contacts, which decreased by about 50% after adding W and C into Cu50Cr, and analyzed the effects of added elements on the welding performance and other properties. In order to improve the dielectric strength of the Cu-Cr electrical contact material, Hasegawa *et al.* [17] added a small amount of Mo in the Cu-Cr alloy, and the dielectric strength along with the anti-welding ability of the contacts were increased dramatically as a result. Furthermore, the in situ formed Al_2O_3 nanoparticles in the copper matrix can effectively enhance the high temperature strength and inhibit the dynamic recrystallization attributed to hindering dislocations movement [18–20]. This has been verified in our previous work [21]. It is demonstrated that the Al_2O_3-Cu/35W5Cr composite was still in the stage of subcrystals formation at 850°C, 0.01 s^{-1} thermal deformation condition. As mentioned above, aluminum oxide dispersion strengthened copper is widely used in electrical contacts, lead frame materials and resistance welding electrodes [22, 23].

In this work, Al_2O_3-Cu/15W and Al_2O_3-Cu/15W5Cr composites were fabricated by vacuum hot-pressing sintering and internal oxidation methods. The microstructure of the Al_2O_3-Cu/15W5Cr composite was analyzed. The effects of Cr on the comprehensive properties, arc erosion morphology and welding force of the electrical contacts were investigated. The mass transfer mechanism was also discussed.

2 Experimental procedure

W powder (5 μm average diameter, >99.9% purity), Cr powder (44 μm average diameter, >99.9% purity) and Cu-0.4wt.%Al powder (2-5 μm diameter, >99.9% purity) were employed. Cu_2O powder (2-5 μm diameter, >99.9% purity) served as the oxygen source. The morphology of different powder and the mixed powder is shown in Figure 1. Powders were adequately mixed in the YH-10 mixer for 2 hours, and the copper ball-to-powder weight ratio was 10:1. The composite samples were sintered using the ZMY-50-15 vacuum hot-press sintering furnace at 3-4 Pa vacuum and 950°C (10°C/min heating rate) with 1 h dwelling time. When the temperature reached 650°C, 15 MPa uniaxial contact pressure was applied for 1 h.

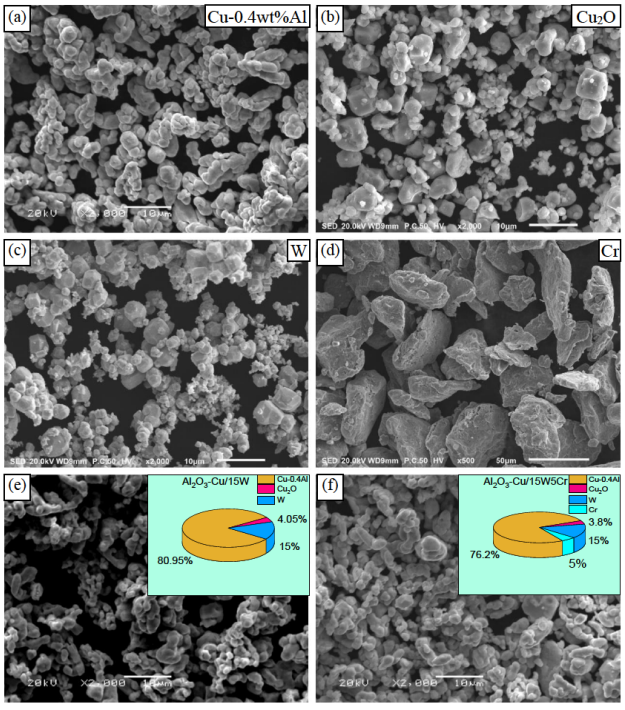

Figure 1: SEM images of the feedstock powder: (a) Cu-0.4 wt.% Al powder; (b) Cu_2O powder; (c) W powder; (d) Cr powder; (e) Mixed powder of Al_2O_3-Cu/15W; (f) Mixed powder of Al_2O_3-Cu/15W5Cr

The relative density was obtained by dividing the bulk density by the theoretical density after the bulk density of the composites was measured by the Archimedes method. Then the Sigma 2008B1 digital instrument was used to measure the electrical conductivity of the as-sintered samples. In order to investigate the microstructure of the composites, the field emission scanning electron microscope (JSM-7800F) and the transmission electron microscope (JEM-2100) were employed.

As-sintered composites were cut into Φ3.8 mm × 10 mm size cylindrical specimens. The specimen surfaces were ground and polished for the following tests. Then the specimens were weighed by the FA2004B electronic balance before and after the predetermined operations, with each data point representing the average value of five measurements. The mass transfer and the loss of the contacts suffering arc erosion, Δm, was calculated as follows: $\Delta m = m_2 - m_1$, where m_2 is the electrode mass after electrical contact testing and m_1 is the specimen mass before electrical contact testing. Five thousand contact cycles were performed on the JF04C electrical contact testing apparatus.

These tests were conducted under the argon atmosphere. The bottom contact was stationary and served as a cathode, while the top contact served as an anode, which was movable. The test was carried out in the constant current mode with the voltage set to 30 V DC and the current set to 10, 20, 25, and 30 A. The contact force was 0.4-0.6 N and the contact breaking frequency was 1 Hz. Three samples were tested for each condition to obtain repeatable experimental results. The arc erosion morphology of the contacts was analyzed by the JSM-5610LV scanning electron microscope.

3 Results

3.1 Microstructures of the composites

Figure 2(a-f) show the SEM images of the Al_2O_3-Cu/15W and Al_2O_3-Cu/15W5Cr composites. As shown in Figure 2, W and Cr particles were uniformly distributed on the copper matrix without obvious agglomeration. The as-sintered composites are compact and have no holes or other defects. As can be seen from the linear scan results in Figure 2(e) and Figure 2(f), the interfaces between W and Cu are obvious, and they are not mutually soluble with a transition layer between Cu and Cr.

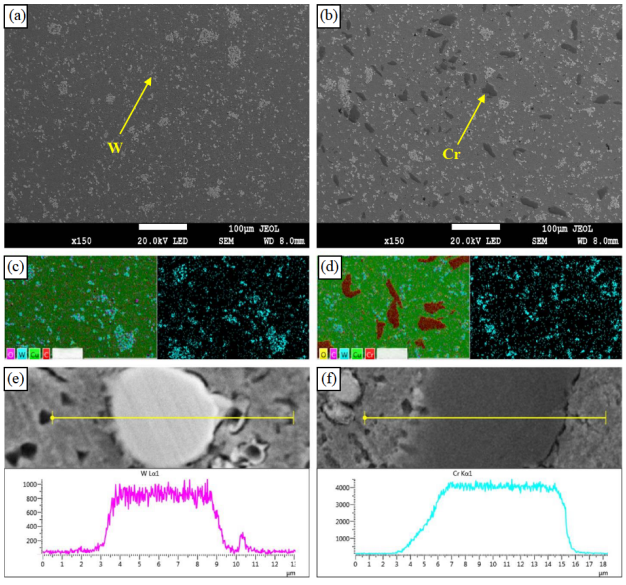

Figure 2: SEM images, corresponding EDS maps at high magnification and element line scans. (a, c) Al_2O_3-Cu/15W composite; (b, d) Al_2O_3-Cu/15W5Cr composite; (e) W particle line scan; (f) Cr particle line scan

Figure 3 and Figure 4 show the TEM characterization of the Al_2O_3-Cu/15W5Cr composite. As seen in Figure 3(a), many nanoparticles are dispersed uniformly in the copper matrix. Selected electron diffraction spots are shown in Figure 3(b), indicating that there is a set of spots of the secondary phase in addition to the {103} zone axial spots of the Cu matrix. Based on the diffraction spots analysis shown in Figure 3(d), it is the diffraction spots of γ-Al_2O_3 along the {103} zone axis. Furthermore, the two sets of diffraction spots in Figure 3(d) disclose an orientation relationship of $<103>_{Cu}//<103>_{\gamma-Al2O3}$, $\{020\}_{Cu}//\{040\}_{\gamma-Al2O3}$. Central dark field observation (shown in Figure 3(c)) was conducted using the secondary phase spot (marked by the circle in Figure 3(b)), and the results showed that all the secondary phase particles generated in the Cu matrix were γ-Al_2O_3.

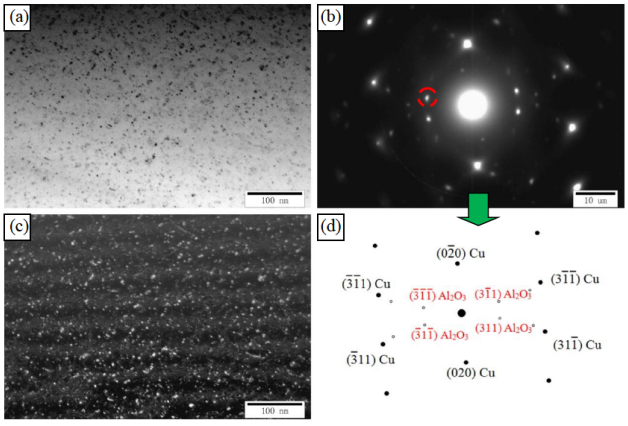

Figure 3: A special orientation relationship of Cu matrix and nano-Al_2O_3 particles. (a) Bright field image; (b) Selected electron diffraction spots; (c) Dark field image; (d) Index of the diffraction spots

It is interesting to note that Al_2O_3 nanoparticles pinned dislocations and hindered the dislocations movement, as shown in Figure 4(a). This phenomenon can be used to explain good mechanical properties of the dispersion copper under high temperature [24–27]. Previous work demonstrated that the Al_2O_3-Cu/35W5Cr composite was still in the stage of sub-crystals formation at 850°C, 0.01 s^{-1} deformation condition. The Al_2O_3-Cu/35W5Cr composite had typical dynamic recovery characteristics [21]. Figure 4(b) shows that twins were formed in the process of hot press sintering. It is well known that the twins' structure reduces the dislocation slip of the average free path, thus effectively promoting hardening [28–30]. Thus, they can enhance the dislocation density and composite hardness. In addition, some Cr particles were

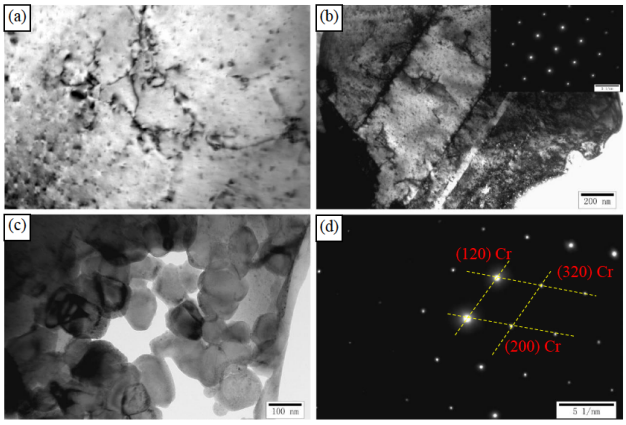

Figure 4: TEM characterization of the Al_2O_3-Cu/15W5Cr composite. (a) Nano-Al_2O_3 particles pinned dislocations; (b) Twins; (c) Fine Cr particles; (d) Selected electron diffraction spots

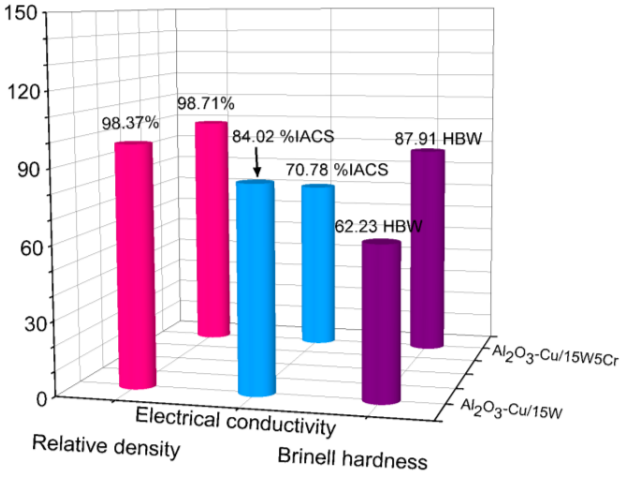

Figure 5: Comprehensive properties of the composites

transformed into fine particles during the vacuum hot-pressing sintering process, shown in Figure 4(c-d).

3.2 Comprehensive properties

The comprehensive properties of the two composites are shown in Figure 5. The relative density of the two composites is above 98%, which can satisfy the basic requirements of electrical contact materials. As the 5 wt% chromium was added to the Al_2O_3-Cu/15W composite, the electrical conductivity decreased, while the Brinell hardness obviously increased. This is because poor interface bonding increases electron scattering. Besides, the electrical conductivity of Cr is lower than copper. However, as a hard phase, Cr can carry and transfer the applied load in the composite material. Additionally, the thermal mismatch between the

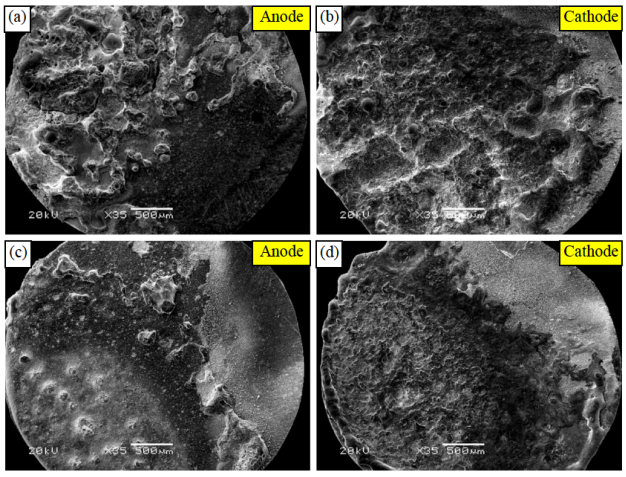

Figure 6: SEM low magnification images of arc erosion of: (a, b) Al_2O_3-Cu/15W composite and (c, d) Al_2O_3-Cu/15W5Cr composite

matrix and Cr particles can increase the hardness of the composite [31, 32].

3.3 Arc erosion morphology

The low-magnification SEM images of the Al_2O_3-Cu/15W and Al_2O_3-Cu/15W5Cr composites are shown in Figure 6. All kinds of hills and craters are present on the anode and cathode surfaces, respectively. It could be found that the anode of Al_2O_3-Cu/15W5Cr composite (Figure 6(c)) contains fewer hills than the Al_2O_3-Cu/15W composite. Moreover, the cathode in Figure 6(d) has fewer craters. It is well established that the increase of Cr content improves contact arc erosion resistance. The solubility of chromium in copper increases to rather high values with temperature resulting in the homogeneous melt on the contacts surface [33, 34].

Figure 7 shows the high-magnification SEM images of the Al_2O_3-Cu/15W5Cr composite and corresponding EDS results after electrical contact test at 30V DC, 30 A. As shown in Figure 8, filaments, needle-like skeletons, droplets, and coral structures were present on the surface of the contacts. In Figure 7(e), EDS data show that the content of copper in the filaments is 88.42 wt%. The reasons for filaments generation are as follows: due to the high temperature of the arc, a liquid bridge was formed between the contacts. At the initial stage of contacts parting, molten metal bridges the contact gap [35, 36]. As the breaking of contacts continued, the gap became wider. Finally, the rupture and solidification of the molten metal bridge took place. Figure 7(b) shows many needle-like skeletons with a diameter less than 1 μm and a length of about 5 μm. Simi-

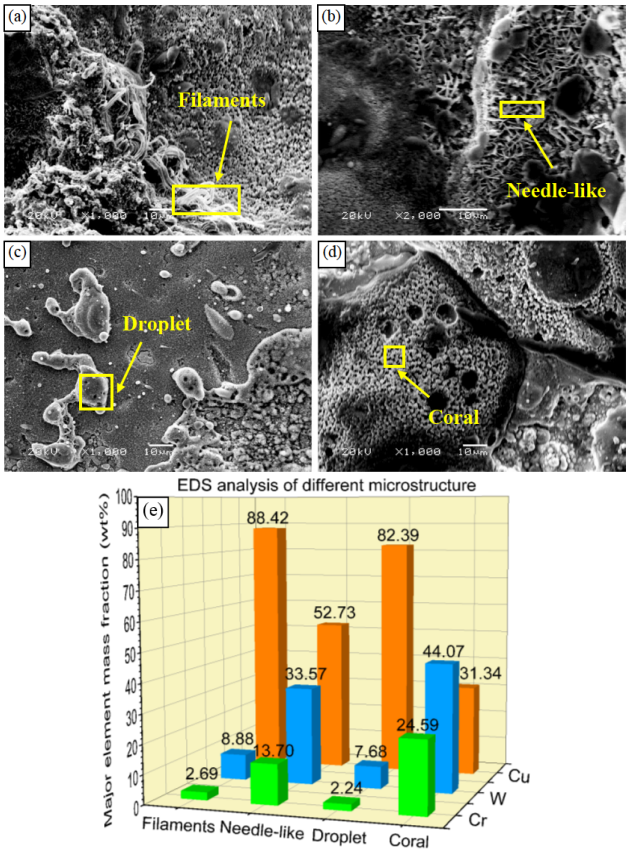

Figure 7: High magnification SEM images of arc erosion morphology and elemental analysis of four boxed areas. (a) Filaments; (b) Needle-like; (c) Droplet; (d) Coral; (e) EDS data

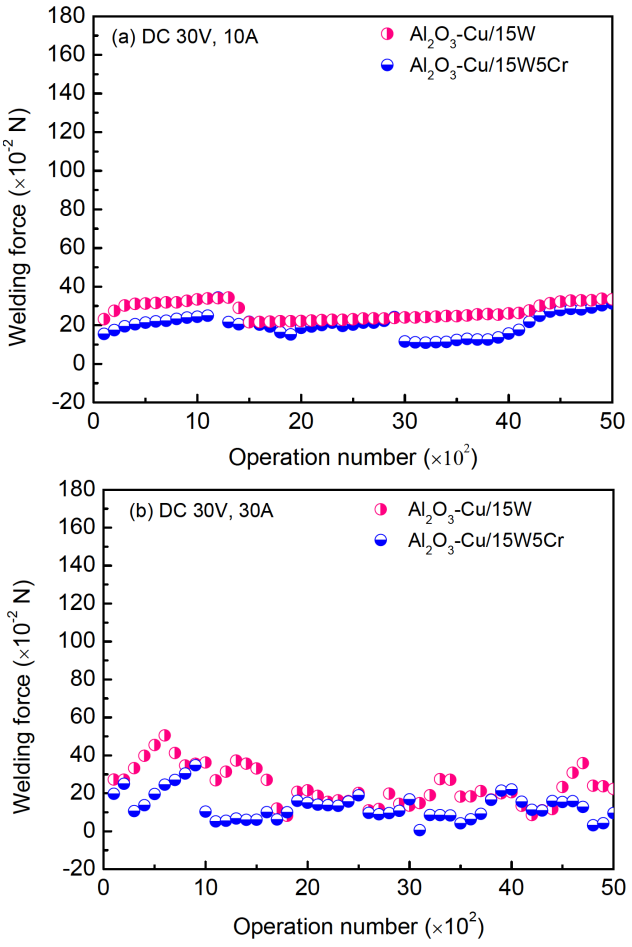

Figure 8: The welding forces of different composites at (a) DC 30V, 10A and (b) 30V, 10A

lar structure has been observed in our previous work. However, the length of the needle was about 10 μm [37]. The EDS data show that the tungsten and chromium content is 33.57 wt% and 13.7 wt%, respectively. This is far more than that in the as-sintered samples. These needle-like structures can restrict the flow of liquid and thus reduce the splashing of materials. In addition, Figure 7(c) shows that some droplets with a copper content as high as 82.39 wt% were scattered on the contact. These droplets were formed by the rapid solidification of liquid copper after splashing. Besides, many coral structures were found in Figure 7(d), which have much higher tungsten and chromium content than the needle-like skeletons. This phenomenon can be explained by the melted copper evaporation and sputter at high temperature. Finally the refractory components tungsten and chromium accumulated to form the coral structures.

3.4 Welding resistance

The arc generated in the process of making and breaking electrical contacts results in material transfer and welding between the electrodes [38, 39]. Figure 8 shows the welding forces of Al_2O_3-Cu/15W and Al_2O_3-Cu/15W5Cr contact materials at DC 30 V, 10 A and 30 A, with each data point representing the average value of 100 breaking operations. The contacts with chromium added under both test conditions have lower welding force. This can be explained by the formation of finely dispersed chromium particles, which prevented generating very hot spots [40]. Furthermore, the contacts with added chromium have a thinner and brickle melted layer. In addition, as can be seen from Figure 7(b, d) that tungsten and chromium underwent a re-sintering process under high temperature and transformed into needle-like and coral structures. These typical structures also contribute to better welding resistance [41–43].

4 Discussion

In general, an arc generation is attributed to the electrical breakdown of a vacuum gap with ample power supplement. Under the action of the arc, the contact temperature increases due to the arc heat flux. In addition, various forces, such as electrostatic force and electromagnetic force, are applied to the contacts. Consequently, the electrical contact material, which has lower melting point melts, evaporates and sprays at first. All kinds of asymmetry factors in the making and breaking process of contacts result in the material transfer or loss [44–46]. Furthermore, material transfer or loss eventually lead to electrical contacts failure. Figure 9 shows the material transfer trend of the two contact materials after 5000 make-and-break tests. As shown in Figure 9(a), the anode mass increases and the cathode mass decreases from 10 A to 30 A consistently. Nevertheless, the Al_2O_3-Cu/15W composite presents two distinct trends before and after 25 A. From 10 A to 25 A, the mass loss value increases with the current, while the mass loss value at 30 A is less than at 25 A, *i.e.*, the 25 A is a critical current value for the material transfer. According to Figure 9(a), all the total mass change values were negative, *i.e.*, the anode mass gain was not equal to the cathode mass loss. This indicates a mass loss to the environment. For comparison in Figure 9(b), the Al_2O_3-Cu/15W5Cr composite shows a similar mass change trend with Figure 9(a). However, the mass change value under all the conditions from 10 A to 30 A is less than in Figure 9(a). This demonstrates that the addition of Cr can reduce the mass transfer of the contacts. Furthermore, the mass change characteristics are totally different between 10-25 A and 25-30 A for both the composites. The specific reasons are analyzed as follows.

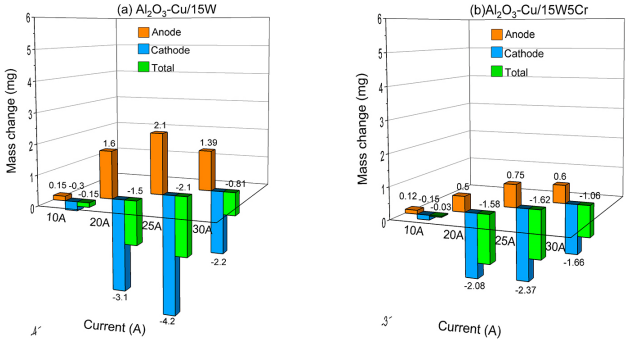

Figure 9: Mass change of the two composites. (a) Al_2O_3-Cu/15W; (b) Al_2O_3-Cu/15W5Cr.

In the first stage from 10 A to 25 A, less charged particles were generated by collision and thermal ionization due to the less heat flux of the arc column. In order to maintain the arc, electrons need to be emitted from the cathode. Positive ions accumulating in the cathode surface area resulted in the higher electric field intensity. At the same time, the arc constriction in the cathode area increased the current density. Hence, more particles near the cathode were ionized. In summary, positive ions accumulated and arc constriction in the cathode area enhanced the heat flux, which was input into the cathode. As a result, the material transferred from the cathode to the anode. On the other hand, the number of charged particles, such as gas molecule and metal vapor atoms at 30 A, was higher than at 25 A. Thus, the probability of collision ionization and thermal ionization increased [47–50]. Maintaining the arc no longer depends on arc constriction in the cathode area and ionization of the electrons, which were emitted from the cathode. Then the arc constriction phenomenon in the cathode area disappeared. In order to maintain the arc and the lowest arc voltage, the arc column in the anode area was constricted. These two processes are illustrated in Figure 10. Heat flux input into the anode contact resulted in the material transfer from the anode to the cathode. Although the material transfer direction changed, the material transferred from the cathode to the anode dominated the final transfer direction. Therefore, the mass change value at 30 A is less than that at 25A.

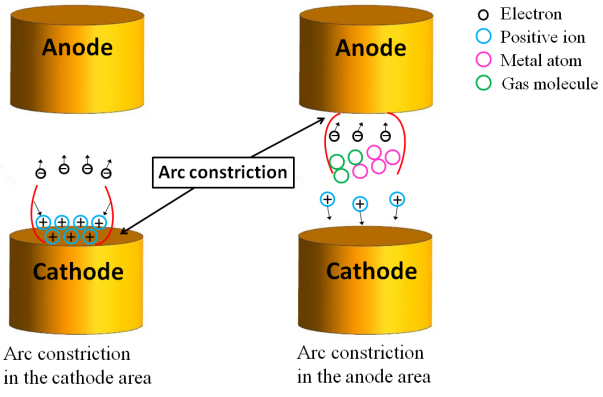

Figure 10: Schematic of the different particles movement under different conditions

5 Conclusions

Vacuum hot-press sintering process was employed to fabricate the Al_2O_3-Cu/15W and Al_2O_3-Cu/15W5Cr composites. W and Cr particles were uniformly distributed in the dispersion copper matrix without obvious agglomeration. The diffraction spots of the Cu matrix and the γ-Al_2O_3 disclose an orientation relationship of $<103>_{Cu}//<103>_{\gamma-Al2O3}$, $\{020\}_{Cu}//\{040\}_{\gamma-Al2O3}$. Al_2O_3 nanoparticles pinning dislocations and twins were clearly observed. During the arc erosion, hills and craters were formed on the anode and cathode surfaces, respectively. Moreover, typical arc erosion morphology, such as needle-like and coral structures were formed, which significantly enhanced arc erosion resistance of the contact material. Compared with the Al_2O_3-Cu/15W composites, the Al_2O_3-Cu/15W5Cr composites have a lower welding force. Furthermore, the two composites present two distinct mass transfer trends before and after 25 A. From 10 A to 25 A, the mass loss value increases with the current, while the mass loss value at 30 A is less than at 25 A. The final mass transfer direction of the composites is from the cathode to anode. The Al_2O_3-Cu/15W5Cr contacts have less mass change under all testing conditions.

Acknowledgement: This work was supported by the Open Cooperation Project of Science and Technology of the Henan Province (182106000018), the Henan University Scientific and Technological Innovation Talent Support Program (18HASTIT024) and the National Natural Science Foundation of China (U1704143).

References

[1] Zhou Z.Y., Zhao L., Sun W.Z., Ni Q.L., Arc development of triggered vacuumswitch with multi-rod electrode system, Instrum. Experim. Techniq., 2016, 59, 84-90.

[2] Slade P. G., The Vacuum Interrupter: Theory, Design, and Application. Boca Raton, FL, USA: CRC Press, 2008.

[3] Scholfield D.W., Buther M.D., Hilko B., Dorr G., Vacuum switch performance in a 1.2 MJ pulse forming network, Review of Scientific Instruments, 2008, 79, 1-5.

[4] Wu C.P., Yi D.Q., Weng W., Li S.H., Zhou J.M., Influence of alloy components on arc erosion morphology of Ag/MeO electrical contact materials, Transactions of Nonferrous Metals Society of China, 2016, 26, 185-195.

[5] Klinski-Wetzel K.V., Kowanda C., Heilmaier M., Mueller F.E.H., The influence of micro-structural features on the electrical conductivity of solid phase sintered CuCr composites, Journal of Alloys and Compounds, 2015, 631, 237-247.

[6] Slade P.G., Electrical contacts: principles and applications, Florida: The Chemical Rubber Company Press, 2013, 233-234.

[7] Guo Z.Q., Geng H.R., Feng S.S., Study on mechanical properties and physical properties of copper based electrical contact materials reinforced by CNT, Advanced Materials Research, 2010, 139-141, 67-71.

[8] Huang X.C., Feng Y., Qian G., Liu K., Erosion behavior of Ti_3AlC_2 cathode under atmosphere air arc, Journal of Alloys and Compounds, 2017, 727, 419-427.

[9] Gao J.R., Liu K., Ai X., Wang X.J., Shi X.Y., Li G., Wang W.B., Electronic beam surface remelting of Cu-Cr contactmaterials, in: Proc 26th IEEE Discharges and Electrical Insulation in Vacuum, 2014, 469-472.

[10] Zhao L.J., Li Z.B., Zhou Y.W., Arc erosion characteristics of nanocrystalline CuCr contact material, in: Proc 1 th IEEE International Conference on Electric Power Equipment-switching Technology, 2011, 594-597.

[11] Zhu S.X., Liu Y., Tian B.H., Zhang Y., Song K.X., Arc erosion behavior and mechanism of Cu/Cr20 electrical contact material, Vacuum, 2017, 143, 129-137.

[12] Schulman M.B., Slade P.G., Loud I.D., Li W., Influence of contact geometry and current on effective erosion of Cu-Cr, Ag-WCand Ag-Cr vacuum contact materials, IEEE Holm Conference on Electrical Contacts, 1998, 307-315.

[13] Mahir U., Usca U.A., Effect of Cr particulate reinforcements in different ratios on wear performance and mechanical properties of Cu matrix composites, Journal of the Brazilian Society of Mechanical Sciences and Engineering, 2018, 40, 197.

[14] Taylor E.D., Cathode spot behavior on Tungsten –copper contact in vacuum and the effect on erosion, IEEE 51th Holm Conference on Electrical Contacts, 2005, 135-138.

[15] Miao B.H., Guo H., Zhang Y., Liu G.X., Effects of interface characteristics of Cu/Cr phases on the contact performance of Cu-25Cr alloy contact material, IEEE 2008 XXIII International Symposium on Discharges and Electrical Insulation in Vacuum, 2008, 185-188.

[16] Chang Y.L., Zheng W., Zhou Z.M., Zhai Y.X., Wang Y.P., Preparation and performance of Cu-Cr contact materials for vacuum switches with low contact pressure, Journal of Electronic Materials, 2016, 45, 5647-5654.

[17] Hasegawa K., Hayashi S., Ishikawa K., Yamamura K., Komatsu H., Furuhata T., Development of Cu-Cr-Mo contact material for vacuum interrupters, International Conference on Electric Power Equipment-Switching Technology, 2016, 90-94.

[18] Tian B.H., Liu P., Song K.X., Li Y., Liu Y., Ren F.Z., Su J.H., Microstructure and properties at elevated temperature of a nano-Al_2O_3 particles dispersion-strengthened copper base composite. Material Science and Engineering A, 2006, 435-436, 705-710.

[19] Dalirbod A., Sorkhe Y.A., Aghajani H., Mechanical properties and fracture study of alumina dispersion hardened copper-based nano-composite at elevated temperatures, Advanced Materials Research, 2014, 829, 583-588.

[20] Song K., Guo X., Liang S., Zhao P., Zhang Y., Relationship between interfacial stress and thermal expansion coeflcient of copper–matrix composites with different reinforced phases, Materials Science and Technology, 2014, 30, 171-175.

[21] Zhang X.H., Zhang Y., Tian B.H., Jia Y.L., Liu Y., Song K.X., Volinsky A.A., Thermal deformation behavior of the Al_2O_3-Cu/(W, Cr) electrical contacts, Vacuum, 2019, 164, 361-366.

[22] Lee D.W., Tolochko O., Choi C.J., Kim B.K., Aluminium oxide dispersion strengthened copper produced by thermochemical process, Powder Metallurgy, 2002, 45, 267-270.
[23] Yue C.F., Chen H.D., Liu G.Y., Lei Z.F., Microstructure and property research of Al_2O_3 dispersion strengthened copper alloy, Rare Metal Materials & Engineering, 2012, 41, 510-513.
[24] Zhang Z., Chen D.L., Consideration of Orowan strengthening effect in particulate-reinforced metal matrix nanocomposites: A model for predicting their yield strength, Scripta Materialia, 2006, 54, 1321-1326.
[25] Zhang Y., Tian B.H., Volinsky A.A., Chen X.H., Sun H.L., Chai Z., Liu P., Liu Y., Dynamic recrystallization model of the Cu-Cr-Zr-Ag alloy under hot deformation, Journal of Materials Research, 2016, 31, 1275-1285.
[26] Simchi H., Simchi A., Tensile and fatigue fracture of nanometric alumina reinforced copper with bimodal grain size distribution, Materials Science & Engineering: A, 2009, 507, 200-206.
[27] Bera S., Lojkowsky W.M., Development of wear-resistant Cu-10Cr-3Ag electrical contacts with alloying and high pressure sintering, Metal Mat Trans A Phys Metall Mat Sci, 2009, 40, 3276-3283.
[28] Mu S.J., Tang F., Gottstein G., A cluster-type grain interaction deformation texture model accounting for twin-induced texture and strain-hardening evolution: Application to magnesium alloys, Acta Materialia, 2014, 68, 310-324.
[29] Radetic T., Radmilovic V., Soffa W.A., Electron microscopy observations of deformation twinning in a precipitation hardened copper-titanium alloy, Scripta Materialia, 1996, 35, 1403-1409.
[30] Wang B.J., Zhang Y., Tian B.H., Yakubov V., An J.C., Volinsky A.A., Liu Y., Song K.X., Li L.H., Fu M., Effects of Ce and Y addition on microstructure evolution and precipitation of Cu-Mg alloy hot deformation, Journal of Alloys and Compounds, 2019, 781, 118-130.
[31] Chawla N., Shen Y.L., Mechanical behavior of particle reinforced metal matrix composites, Advanced Engineering Materials, 2001, 3, 357-370.
[32] Raabe D., Miyake K., Takahara H., Processing, microstructure, and properties of ternary high-strength Cu–Cr–Ag in situ composites, Materials Science & Engineering A, 2000, 291, 186-197.
[33] Lin R.J., Wang L.J., Shi W.X., Deng J., Jia S.L., Experimental investigation on triggered vacuum arc and erosion behavior under different contact materials, IEEE Transactions on Plasma Science, 2018, 46, 3047-3056.
[34] Li W.P., Thomas R.L., Smith R.K., Effects of Cr content on the interruption ability of CuCr contact materials, IEEE Transactions on Plasma Science, 2001, 29, 744-748.
[35] Laurent M., Nouredine B.J., Didier J., Make Arc erosion and welding in the automotive area, IEEE Transactions on components and packaging technologies, 2000, 23, 240-246.
[36] Slade P.G., Nonmember, Opening electrical contacts: The transition from the molten metal bridge to the electric arc, IEICE Trans. Electron, 2010, E93-C, 1380-1386.
[37] Zhang X.H., Zhang Y., Tian B.H., An J.C., Zhao Z., Volinsky A.A., Liu Y., Song K.X., Arc erosion behavior of the Al_2O_3-Cu/(W, Cr) electrical contacts, Composite Part B, 2019, 160, 110-118.
[38] Li W.J., Shao W.Z., Xie N., Zhang L., Li Y.R., Yang M.S., Chen B.A., Zhang Q., Wang Q., Zhen L., Air arc erosion behavior of $CuZr/Zn_2SnO_4$ electrical contact materials, Journal of Alloys and Compounds, 2018, 743, 697-706.
[39] Neuhaus A.R., Rieder W.F., Hammerschmidt M., Influence of electrical and mechanical parameters on contact welding in low power switches, IEEE Transactions on Components and Packaging Technologies, 2004, 27, 4-11.
[40] Heitzinger F., Kippenberg H., Saeger K.E., Schroder K.H., Contact materials for vacuum switching devices, IEEE Transactions on Plasma Science, 1993, 21, 447-453.
[41] Liu X.J., Fei H.J., A new mathematical model of dynamic welding for electric contacts. Transactions of China Electrotechnical Society, 2001, 16, 81-84 (in Chinese).
[42] Yu L., Geng Y.S., Li Q., Wang J.H., Liu Z.Y., Li D.W., Wang W.B., Wang X.J., Improvement of percussion welding characteristics of CuCr25 contact material by decreasing tensile strength, Proceedings of the 55th IEEE Holm Conference on Electrical Contacts, HOLM, 2009, 195-199.
[43] Miao B.H., Zhang Y., Liu G.X., Current status and developing trends of Cu-Cr contact materials for VCB, International Symposium on Discharges & Electrical Insulation in Vacuum, 2004, 311-314.
[44] Boxman R.L., Goldsmith S., Greenwood A., Twenty-five years of progress in vacuum arc research and utilization, IEEE Transactions on Plasma Science, 1998, 25, 1174-1186.
[45] Sawa K., Hasegawa M., Recent researches and new trends of electrical contacts, IEICE Trans. Electron, 2000, E83-C, 1363-1376.
[46] Ding J., Tian W.B., Zhang P., Zhang M., Zhang Y.M., Sun Z.M., Arc erosion of Ag/Ti3AlC2 electrical contact materials, Journal of Alloys and Compounds, 2018, 740, 669-676.
[47] Rong M.Z., Yang Z.Y., Yang W., Contact material transfer of low voltage apparatus, Low Voltage Apparatus, 1998, 5, 16-18.
[48] Chen Z.K., SAWA K., Particle sputtering and deposition mechanism for material transfer in breaking arcs, Journal of Applied Physics, 1994, 76, 3326-3331.
[49] Swingler J., Mcbridle J.W., A comparison of the erosion and arc characteristics of Ag/CdO and Ag/SnO_2 contact materials under DC break conditions, Proceedings 41st IEEE Holm Conference, 1995, 381-392.
[50] Chen Z.K., Sawa K., Effect of arc behavior on material transfer: a review, IEEE Transactions on Components, Packaging, and Manufacturing, Technology, Part A, 1998, 21, 310-322